Non-Uniform Markov Random Fields for Classification of SAR Images

Sylvain Lobry, LTCI, CNRS, Télécom ParisTech, Université Paris-Saclay, sylvain.lobry@telecom-paristech.fr, France
Florence Tupin, LTCI, CNRS, Télécom ParisTech, Université Paris-Saclay, florence.tupin@telecom-paristech.fr, France
Roger Fjørtoft, CNES, roger.fjortoft@cnes.fr, France

Abstract

When dealing with SAR image classification, the class parameters may vary along the swath for several reasons. Traditional classification algorithms are then not well adapted, as they assume constant class parameters. In this paper, we propose a binary classification algorithm based on Markov Random Fields that take into account the parameters variations in the swath, and we present results obtained on airborne TropiSAR and simulated SWOT HR data.

1 Introduction

Because of their robustness with respect to weather and light conditions, synthetic aperture radar (SAR) acquisitions are used for mapping or change detection. These applications often rely on a classification step, which is one of the primary challenges in automated SAR image analysis. This task can be achieved in many ways, e.g. by pixelwise classification with prior speckle filtering, by segmentation followed by region-wise classification [1], by feature extraction and post-processing [14] or directly using Markov Random Fields [13].

In this paper, we propose a binary classification method adapted to class parameters variations along the swath. Such variations can have several origins. For the SWOT mission [7], whose principal instrument is a Ka-band Radar Interferometer (KaRIn) operating at near-nadir incidences (1°-4°), they are mainly due to the antenna pattern, the evolution of the pixel size and the normalized backscattering coefficient with incidence, as well as local variations due to varying surface roughness. Even if we let aside the latter, these variations cannot easily be compensated globally, because the resulting intensity evolution depends on the class: it is not the same for water (strong backscattering in near-nadir) and land surfaces (dominated by the thermal noise floor, which is flat). For the airborne TropiSAR data used in this study, the variations are mainly due to the uncompensated antenna pattern. Our main application is water detection which is an important purpose for the future SWOT mission.

The proposed model is introduced in section 2. An exact optimization method for this model is presented in section 2.3. Finally, we present the results obtained on airborne TropiSAR and simulated SWOT HR data in section 3.

2 Non-Uniform Markov Random Fields

Given a set of pixels $\mathcal{S} = \{s_i, 0 \leq i < N_s\}$, we consider two random processes:

- $\mathbf{V} = (V_s)_{s\in\mathcal{S}}$ modeling the observed image to be classified;
- $\mathbf{U} = (U_s)_{s\in\mathcal{S}}$ modeling the result of the classification.

In the previous definitions the state space are the following: $V_s \in \mathbb{R}$ and $U_s \in \Lambda = \{1, \dots, N_\lambda\}$, with N_λ the number of classes. In the rest of this article, we only consider the case of binary classification (i.e. $N_\lambda = 2$) even though the proposed method could be adapted to multi-label problems.

Realizations of $\mathbf{V}$ and $\mathbf{U}$ are named $\mathbf{v} = (v_s)_{s\in\mathcal{S}}$ and $\mathbf{u} = (u_s)_{s\in\mathcal{S}}$ respectively.

Our goal is to find the realization $\hat{\mathbf{u}}$ of $\mathbf{U}$ that best explains the observation $\mathbf{v}$. Following the work of [8], this can be expressed as:

$$\begin{aligned} \hat{\mathbf{u}} &= \arg\min_{\mathbf{u}} -\log\left(\mathrm{p}(\mathbf{v}|\mathbf{u})\right) - \log\left(\mathrm{p}(\mathbf{u})\right) \\ &= \arg\min_{\mathbf{u}} \mathcal{E}(\mathbf{u}), \end{aligned} \tag{1}$$

involving the likelihood $\mathrm{p}(\mathbf{v}|\mathbf{u})$ of the observation considering the chosen classification and a prior on the classification result $\mathrm{p}(\mathbf{u})$.

2.1 Prior definition

On such classification tasks, a widely used prior is to enforce spatial coherence for the classes between neighbor pixels. When using only 2 labels, a common prior is the Ising model:

$$-\log\left(\mathrm{p}(\mathbf{u})\right) = \sum_{\{s,t\}\in\mathcal{C}} \beta \ \ |u_s - u_t|\,, \tag{2}$$

where $\mathcal{C}$ is the set of all cliques in $\mathcal{S}$ depending on the chosen neighborhood (4 or 8 connectivity) and β is a balancing term, that needs to be tuned by the user.

2.2 Likelihood definition

In the case of intensity SAR images, speckle approximately follows a Gamma distribution [9] and can be considered separable:

$$\mathrm{p}(\mathbf{V}=\mathbf{v}|\mathbf{U}=\mathbf{u}) = \prod_{s\in\mathcal{S}} \mathrm{p}(V_s = v_s|U_s = u_s)\,, \quad (3)$$

The likelihood $\mathrm{p}(V_s = v_s|U_s = u_s)$ is usually chosen for each class i:

$$\mathrm{p}(V_s = v_s|U_s = i) = \frac{1}{\Gamma(L)}\frac{L}{\mu_i}\left(\frac{Lv_s}{\mu_i}\right)^{L-1} e^{-\frac{Lv_s}{\mu_i}}\,, \quad (4)$$

where L is the number of looks of the image and μ_i is the mean of the class i. In case of unsupervised classification, μ_i is not available. It is usually estimated using an iteratively updated classification. Given a previous classification $\mathbf{u}_{prev}$, $\hat{\mu_i}$ is given by the maximum-likelihood estimator:

$$\hat{\mu_i} = \frac{1}{|\mathcal{S}_i|}\sum_{s\in\mathcal{S}_i} v_s\,, \quad (5)$$

where $\mathcal{S}_i = \{s, u_{prev,s} = i\}$.

2.2.1 Iterative parameters estimation

When considering unsupervised classification, equation 5 can not be applied directly. In [6] an iterative method is used to estimate the parameters. This algorithm is summarized in **Figure 1**. It requires an initialization (in the following, we use K-Means algorithm to obtain it), and estimate the parameters from this first classification. A new classification is produced using computed parameters and allows to estimate new parameters. This process is iterated until no change occurs, or for a fixed number of iterations.

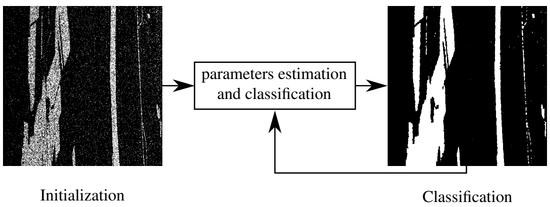

Figure 1: Summary of the method introduced in [6]. Starting from an initialization, two class parameters are estimated and a classification using the described MRF is done. New parameters are estimated from the classification and the process is repeated iteratively.

2.2.2 Class variations

When classes have an important intra-class variation, using only one parameter for each class does not yield good results (see **Figure 5c**). We show the variation of the true mean intensity for water and background classes in a simulated SWOT SAR image in **Figure 2**. This simulation is based on a physical modeling of the surfaces [5] and the parameters are computed using a ground-truth. The red curve shows the mean intensity when computed on the whole image. Compared to the locally computed means, the mean computed on the whole image does not represent any part of the image.

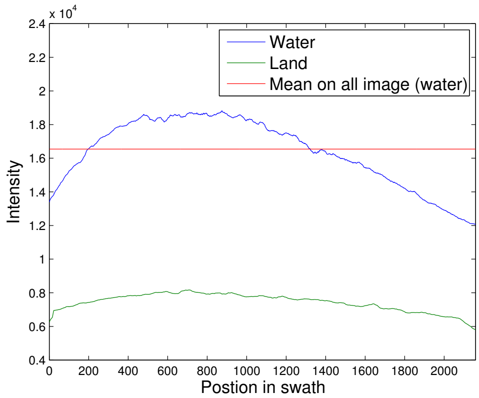

Figure 2: Across-track average intensity for each class in the simulated SWOT image [5] depending on the position in the swath.

To take into account the variations in the image, we propose to use variable parameters for each classes by image partitioning. A summary of the proposed method is shown in **Figure 3**.

Image partitioning We seek a partitioning of the image so that each region fulfills the following requirements:

- It should contain enough pixels of the two classes so that the maximum likelihood estimator is valid ($\mathcal{R}_1$). In practice, a minimal size is fixed (in the following: 2500 pixels) and the least represented class in the region must be over a given percentage (in the following: 10%).
- It should be small enough so there is almost no variation of the parameters in it ($\mathcal{R}_2$). To reach this minimal size, the partitioning is done as long as $\mathcal{R}_1$ is fulfilled.

To obtain such a partition, we propose to use quadtrees [11]. Quadtrees have been extensively used for image coding [12] and segmentation [2].
The partitioning process is as follows:

1. Starting from a region (for the first iteration, the region is the whole image) and a classification (obtained either using a previous classification or K-Means for the first iteration, and the previous classification for the next ones), a partitioning in regions of equal size fulfilling the 2 requirements is searched for the considered region:
   (a) First, we divide the region in 4 (horizontal and vertical cuts).
   (b) If this division breaks one of the requirements, we cancel the previous division and only divide in 2 (vertical cut).

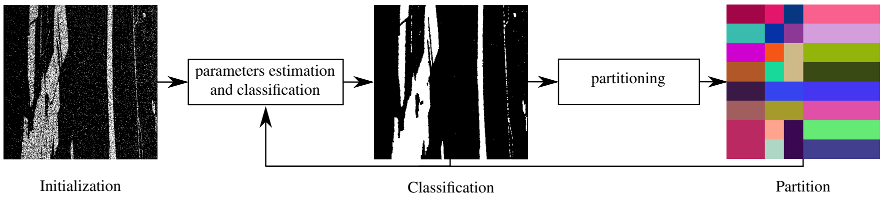

Figure 3: Summary of the proposed method. Starting from an initialization, class parameters are estimated and a classification using the described MRF is done. From this classification, a partitioning is created as described in 2.2.2. New parameters (one for each region and each class) are estimated from the classification and the process is repeated iteratively.

   (c) If this division also breaks one of the requirements, it is canceled, and we try to divide in 2 (horizontal cut).

   (d) If this division also breaks one of the requirements, it is also canceled.

2. If a partition has been performed in the previous steps, the class parameters are updated region-wise and a new classification is computed. The newly created regions are partitioned again starting from step 1.

3. We stop the process when no region can be divided.

Global regularization of the parameters $\mathcal{R}_1$ is checked using a previous classification. If the classification contains wrongly classified pixels, it will impact the following steps. To limit the influence of the initialization, a regularization step enforcing smooth variations along the swath is done.

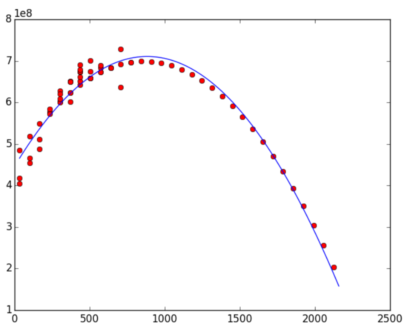

Figure 4: Regularization curve for the parameters of the water class of **Figure 6**.

At each iteration, a Least-Squares Fitting of a continuous function (in our case, a second order polynomial) on the values of the parameters of the regions is performed with respect to the position in the swath of the center of the region.
This allows us to obtain a global trend of the variations of the parameters along the swath. Parameters that are too far from this global trend are likely to be degenerate cases and the parameters are set to the value of the curve at this position. Parameters that are close enough to the value of the curve are kept, allowing for some local variations in the class parameters.

2.3 Optimization

Classical methods used for Markov Random Field optimization such as ICM (iterated conditional modes) and simulated annealing can be used to solve this problem. For a binary classification task, the optimization scheme introduced in [10] can also be used. This method allows to find the global optimum by constructing a graph on which a s-t cut corresponds to a solution to our problem. The global optimum is found using a min-cut algorithm [3] corresponding to the solution of minimum energy. To perform the optimization when using more than 2 classes, α-β swap can be used providing an approximate solution [4].

3 Results

Dataset To illustrate the results of this method we applied it in the framework of water detection on two images:

1. Kaw, French Guiana, TropiSAR dataset acquired by SETHI (airborne sensor of ONERA) in **Figure 5**. P-Band, HH polarization, azimuth resolution: 1.5m, slant-range resolution: 1.2m.

2. Camargue, France, SWOT simulation (2 looks) ([5]) in **Figure 6**. Ka-Band, azimuth resolution: 2m, range resolution from 10 to 60m.

Quantitative criteria For each classification output we show the error rate, which is defined as:

$$\frac{FP + FN}{TP + FN}, \tag{6}$$

where FP is the number of pixels incorrectly classified as water, FN is the number of pixels incorrectly classified as background and TP is the number of pixels correctly classified as water.
For each of these images, we provide the obtained results:

- using the classification (obtained by K-Means) used as an initialization of the algorithms;

- using the classical Markov Random Fields (one parameter for each class, [6] with the exact optimization presented in this paper) with the same number of iterations that were run for the image with the Non-Uniform Markov Random Fields.

- using the proposed method.

Discussion The proposed method greatly improves the results for TropiSAR data compared to the classical Markov Random Fields, but only provides a limited improvement for SWOT images.
This can be explained by the contrast between the extremities of the images and the center of the antenna pattern. This contrast is of 1.56 for the SWOT image, and of 4.79 for the TropiSAR image. With a high contrast between the same class parameters across the image, the classical Markov Random Fields will achieve poor results while the proposed method is able to give better estimates.

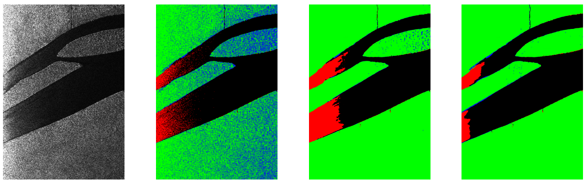

(a) Input image **(b)** Initial classification, error rate = 34.56% **(c)** Uniform MRF, error rate = 11.37% **(d)** Non Uniform MRF, error rate = 4.49%

Figure 5: Results on Kaw area acquired with TropiSAR. Green: true positive, red: false negative, black: true negative and blue: false positive. Input image provided by ESA.

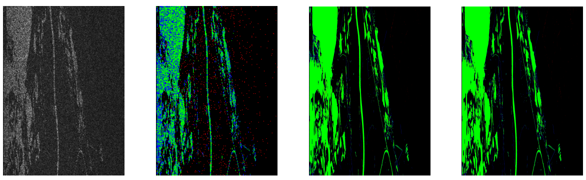

(a) Input image [5] **(b)** Initial classification, error rate = 48.45% **(c)** Uniform MRF, error rate = 5.81% **(d)** Non Uniform MRF, error rate = 5.63%

Figure 6: Extracts of the results obtained on simulated SWOT images of the Camargue area. Green: true positive, red: false negative, black: true negative and blue: false positive.

4 Conclusions

This paper introduces a partitioning-based classification method suited to SAR data presenting variations of the class parameters along the swath. This method can improve the results when dealing with images with an antenna pattern not corrected or other variations in backscattering, for instance like SWOT or TropiSAR data.

Acknowledgment

The authors would like to thank the The European Space Agency (ESA) for the TropiSAR image. This work has been funded by the CNES and the “Future et Ruptures” (Institut Mines-Télécom) program.

References

[1] I. Ben Ayed, A. Mitiche, and Z. Belhadj. Multiregion level-set partitioning of synthetic aperture radar images. *Pattern Analysis and Machine Intelligence, IEEE Transactions on*, 27(5):793–800, 2005.

[2] C. Bouman et al. A multiscale random field model for bayesian image segmentation. *Image Processing, IEEE Transactions on*, 3(2):162–177, 1994.

[3] Y. Boykov and V. Kolmogorov. An experimental comparison of min-cut/max-flow algorithms for energy minimization in vision. *Pattern Analysis and Machine Intelligence, IEEE Transactions on*, 26(9):1124–1137, 2004.

[4] Y. Boykov, O. Veksler, and R. Zabih. Fast approximate energy minimization via graph cuts. *Pattern Analysis and Machine Intelligence, IEEE Transactions on*, 23(11):1222–1239, Nov 2001.

[5] D. Desroches, J.-M. Gaudin, R. Fjortoft, D. Massonnet, J. Duro, and N. Pourthie. Water height restitution without control points proposed for SWOT high rate mode. *Submitted to Geoscience and Remote Sensing, IEEE Transactions on*, 2015.

[6] R. Fjortoft et al. Unsupervised classification of radar images using hidden Markov chains and hidden Markov random fields. *Geoscience and Remote Sensing, IEEE Transactions on*, 41(3):675–686, 2003.

[7] R. Fjortoft et al. KaRIn on SWOT: Characteristics of Near-Nadir Ka-Band Interferometric SAR Imagery. *Geoscience and Remote Sensing, IEEE Transactions on*, 52(4):2172–2185, April 2014.

[8] S. Geman and D. Geman. Stochastic relaxation, gibbs distributions, and the bayesian restoration of images. *Pattern Analysis and Machine Intelligence, IEEE Transactions on*, PAMI-6(6):721–741, Nov 1984.

[9] Joseph W Goodman. *Speckle phenomena in optics: theory and applications*. Roberts and Company Publishers, 2007.

[10] DM Greig et al. Exact maximum a posteriori estimation for binary images. *Journal of the Royal Statistical Society. Series B (Methodological)*, pages 271–279, 1989.

[11] Hanan Samet. The quadtree and related hierarchical data structures. *ACM Comput. Surv.*, 16(2):187–260, jun 1984.

[12] GJ Sullivan and RL Baker. Efficient quadtree coding of images and video. *Image Processing, IEEE Transactions on*, 3(3):327–331, 1994.

[13] Céline Tison, Jean-Marie Nicolas, Florence Tupin, and Henri Maître. A new statistical model for Markovian classification of urban areas in high-resolution SAR images. *Geoscience and Remote Sensing, IEEE Transactions on*, 42(10):2046–2057, 2004.

[14] J.D. Wegner, R. Hansch, A. Thiele, and U. Soergel. Building detection from one orthophoto and high-resolution insar data using conditional random fields. *Selected Topics in Applied Earth Observations and Remote Sensing, IEEE Journal of*, 4(1):83–91, March 2011.